THE ASTROPHYSICAL JOURNAL, 465:L123–L127, 1996 July 10

SYNTHETIC SPECTRA AND MASS DETERMINATION OF THE BROWN DWARF GLIESE 229B

FRANCE ALLARD
Department of Physics, Wichita State University, Wichita, KS 67260-0032; allard@eureka.physics.twsu.edu
PETER H. HAUSCHILDT
Department of Physics and Astronomy, Arizona State University, Box 871504, Tempe, AZ 85287-1504; yeti@sara.la.asu.edu
AND
ISABELLE BARAFFE AND GILLES CHABRIER
Centre de Recherche Astronomique de Lyon (UMR 142 CNRS), Ecole Normale Supérieure, 69364 Lyon Cedex 07, France;
ibaraffe@cral.ens-lyon.fr, chabrier@cral.ens-lyon.fr
Received 1996 February 28; accepted 1996 April 30

ABSTRACT

We present preliminary nongray model atmospheres and interiors for cool brown dwarfs. The resulting synthetic spectra are compared to available spectroscopic and photometric observations of the coolest brown dwarf yet discovered, Gl 229B (Nakajima et al.). Despite the grainless nature of the present models, we find that the resulting synthetic spectra provide an excellent fit to most of the spectral features of the brown dwarf. We confirm the presence of methane absorption and the substellar nature of Gl 229B. These preliminary models set an upper limit for the effective temperature of 1000 K. We also compute the evolution of brown dwarfs with solar composition and masses from 0.02 to 0.065 $M_\odot$. While uncertainties in the age of the system yield some indeterminateness for the mass of Gl 229B, the most likely solution is $m \approx 0.04-0.055\ M_\odot$. In any case, we can set an upper limit $m = 0.065\ M_\odot$ for a very unlikely age, $t = 10$ Gyr.

Subject headings: stars: atmosphere — stars: evolution — stars: fundamental parameters — stars: low-mass, brown dwarfs

1. ABOUT GLIESE 229B

A systematic survey of the nearby stars led by the Caltech–Johns Hopkins University collaboration (Nakajima et al. 1995) has recently achieved a breakthrough in the search for brown dwarfs. With the Johns Hopkins University Adaptive Optics Coronagraph, D. A. Golimowski and B. R. Oppenheimer uncovered the coolest brown dwarf ever found, Gl 229B, which is 10 times fainter than previously known brown dwarf candidates and is orbiting an M1 type dwarf only 5.7 pc from the Earth. Spectra of the object obtained on the Hale 200 inch (5.1 m) telescope by Oppenheimer et al. (1995) and by a number of other investigators reveal unique spectral signatures reminiscent of those seen in Jupiter. If confirmed, the detection of methane bands in Gl 229B could establish beyond doubt the substellar nature of the object.

Recent work by Tsuji, Ohnaka, & Aoki (1996a, 1996b) has revealed the possible influence of grain formation upon the spectroscopic properties of very low mass stars and brown dwarfs. In this paper we show how the various spectroscopic features of Gl 229B can be reproduced only by *grainless* homogeneous models, suggesting that grains either must have sunk below the photosphere over the brown dwarf's lifetime or must be clumped in clouds as suggested by Tsuji et al. (1996b). Despite the proximity of the system, the large orbital separation will not permit a dynamical measure of the mass for at least a decade to come. We therefore use our grainless models to set a meaningful upper limit on the effective temperature and mass for the brown dwarf.

2. BROWN DWARF MODEL ATMOSPHERES

We have constructed a grid of nongray model atmospheres in radiative, convective, and local thermodynamic equilibrium using the stellar atmosphere code Phoenix. Molecular and atomic opacities are treated line by line with van der Waals pressure broadening. Convection is included through the mixing-length approximation. The models are characterized by the following parameters: (1) surface gravity, sampling log $g = 4.0-5.8$; (2) effective temperature, $T_{\rm eff}$, here taken from 1600 to 900 K in steps of 100 K; (3) the ratio l of mixing length to scale height, here taken to be unity; (4) microturbulent velocity ξ, here set to $\xi = 2$ km s^{-1}; and (5) the elemental abundances, which we set to solar values (Grevesse & Noels 1993). Inhomogeneities such as the formation of clouds and effects of condensation and grain opacities are not included in the models at this point.

This grid provides an extension of the red dwarf work by Allard et al. (1994) and Allard & Hauschildt (1995, hereafter AH95) to the brown dwarf realm. Pertinent additions to Phoenix since AH95 include (1) an upgrade of the equation of state (EOS) from 98 to 206 molecules using the polynomial partition functions by Irwin (1988); (2) the addition of H_3^+ and H_2^+ from Neale & Tennyson (1995) and Neale, Miller, & Tennyson (1996) to both the EOS and the opacities; (3) the use of the TiO line list from Jørgensen (1994); (4) the use of the H_2O line list from Miller et al. (1994); (5) the inclusion of IR rotational collision–induced absorption (CIA) of H_2 by Zheng & Borysow (1994); (6) the inclusion of the IR rotovibrational system of SiO by Langhoff & Bauschlicher (1993); and, finally, (7) the incorporation of the HITRAN and GEISA molecular transitions data banks for 31 molecules, including CH_4 and NH_3 from Rothman et al. (1992) and Husson et al. (1992), respectively.

The limitations of the HITRAN and GEISA data banks with respect to methane have been discussed in detail by Strong et al. (1993). These databases were originally intended

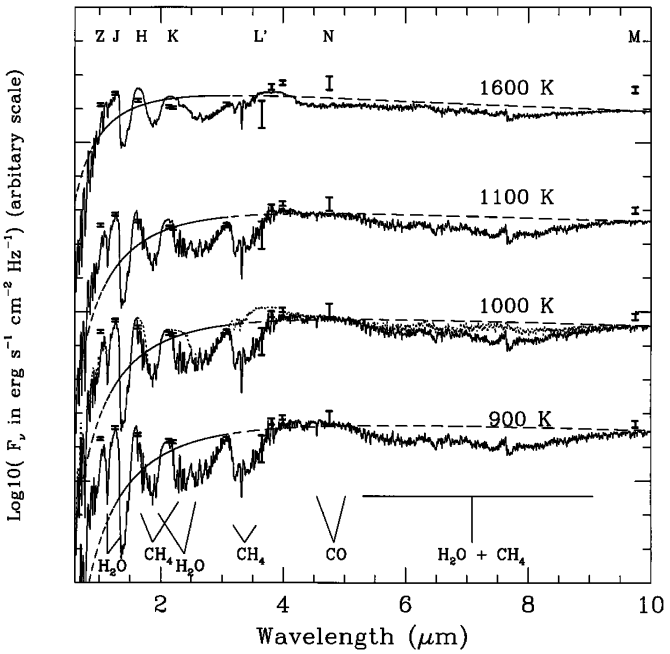

FIG. 1.—Synthetic flux distributions of brown dwarfs with $T_{\rm eff}$ between 1600 and 900 K, log g = 5.0, and assumed solar metallicity (*solid lines*) are compared to the latest broadband photometry (shown with error bars) of Gl 229B (K. Matthews et al., IAU Circ. 6280). A methane-less spectrum (*dotted lines*) is shown for one of the models (1000 K) to emphasize the position of these bands. The photometric fluxes are normalized to each model at the peak of the *J*-band flux. Blackbody distributions of the same effective temperatures are also shown (*dashed lines*) for comparison.

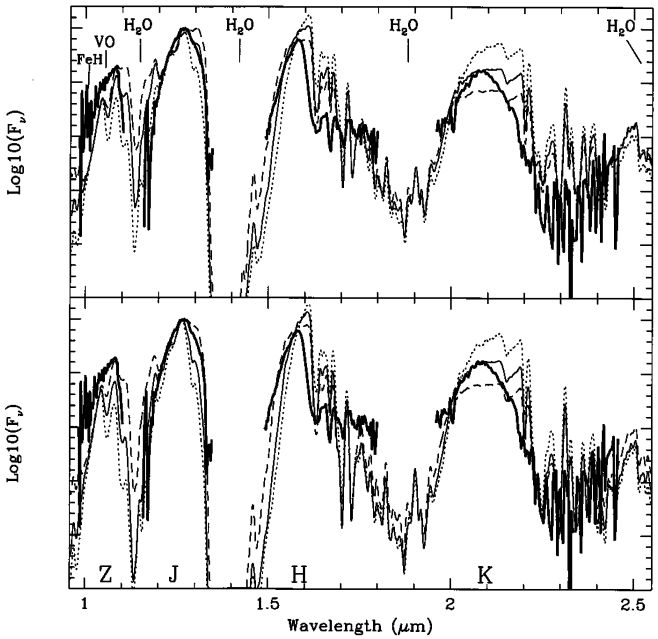

FIG. 2.—Observed spectrum of Gl 229B (*thick lines*) compared to two $T_{\rm eff}$ series of solar composition models of varying gravity. The $T_{\rm eff}$ = 1000 K sequence (*upper panel*) ranges from log g = 4.5 (*dotted lines*) to log g = 5.8 (*dashed lines*), with the best fit reached for 5.3 (*thin solid lines*). The $T_{\rm eff}$ = 900 K sequence (*lower panel*) ranges from log g = 4.0 (*dotted lines*) to log g = 5.5 (*dashed lines*), with the best fit reached for 4.8 (*thin solid lines*). Models and observations have been renormalized in each window to unity at the peak of the *J* bandpass. Two methane systems not explicitly indicated on the plot are seen in this range at 1.6–1.8 μm and at 2.2–2.5 μm.

for Earth atmosphere applications and contain only the strongest (about 47,000) of the millions of transitions expected for this molecule under stellar gas conditions which would provide a pseudo-"continuum" for the bands. We nevertheless include these in the present preliminary models as a diagnostic of the presence of methane bands in the atmospheres. More accurate models will require a calculation of the CH_4 molecule from first principles. To date, only one such calculation exists, which lists CH_4 lines only redward of about 3 μm (Tyuterev et al. 1994).

3. SPECTRAL ANALYSIS

3.1. *Temperature and Surface Gravity of Gliese 229B*

The most reliable way of determining the effective temperature of a cool dwarf is by fitting its overall spectral distribution. In Figure 1 we compare the latest infrared broadband fluxes by T. Nakajima (IAU Circ. 6280) to our models at four temperatures between 1600 and 900 K (i.e., surface temperatures of 700–400 K) at a constant gravity of log g = 5.0. Water vapor, which only condenses from the gas phase at about 300–373 K, dominates the entire infrared spectral distribution in Figure 1. Note, however, that methane absorption breaks through the water continuum in the *H* and *K* bandpasses, and near 3.4 μm at effective temperatures below 1600 K (the upper range of our models). Since a star at the hydrogen-burning limit has an effective temperature of about 2000 K (Baraffe et al. 1995), methane which is particularly obvious in the *L'* band spectral region therefore clearly reveals the substellar nature of Gl 229B. We draw particular attention to the spectral range from about 3.5 to 5 μm, where four bandpasses sample a region over which our models are especially temperature sensitive. The 4.3–5.2 μm CO bands dominate this spectral region in cool M dwarfs and "hot" brown dwarfs, disappearing at lower temperatures as CH_4 and CO_2 gradually form at the expense of CO. Therefore, cooler brown dwarf models ($T_{\rm eff}$ < 1000 K) are left with a much broader peak around 4.5 μm. The observed *L'*- and *N*-band fluxes indicate that no CO absorption is seen in Gl 229B, and 1000 K is the hottest model that lies within the *N*-band error bar, regardless of gravity. Furthermore, the fact that the *M* and *N* fluxes are still above our coolest model suggests that Gl 229B is even cooler than 900 K, and more flux redistribution is needed to match these bandpasses. However, it is possible that these fluxes are still affected by uncertainties in the calibration.

In Figure 2 we compare our 1000 and 900 K models to the Hale spectrum of Gl 229B, recently recalibrated by Matthews et al. (1996). The locations of all the major absorption features of Gl 229B are relatively well reproduced by the models. The agreement is better in spectral ranges dominated by water, i.e., in the *J* bandpass and in the blue wing of the *K* bandpass. For the temperatures occurring in the atmospheres of brown dwarfs (400 K ≤ T ≤ 2000 K in this model grid), the H_2O opacities adopted here (as prescribed by Schryber, Miller, & Tennyson 1995) appear adequate to describe the data. The intrinsic temperature sensitivity of the water opacity profile in this spectral range results in a strong response of the *K* bandpass flux to changes in the atmospheric structure, causing the models to be quite sensitive to gravity in the *K* bandpass

flux. We find that the K/J flux ratio can equally be satisfied by temperature and gravity pairings of $T_{\rm eff} = 1000$ K, $\log g = 5.3$ (Fig. 2, *upper panel*) or 900 K, $\log g = 4.8$ (Fig. 2, *lower panel*). Yet the width of the J bandpass flux, which is shaped by H_2O opacities, is best reproduced by the former solution. Missing methane transitions and flux calibration uncertainties in the H and K bandpasses can easily account for the remaining discrepancies and amount to a 0.2 dex error in each gravity estimate.

3.2. *The Role of Grains and Condensation in Gliese 229B*

Our solar mix models predict strong absorption bands of VO and FeH blueward of 1.1 μm that are not observed in the spectrum of Gl 229B (see Fig. 2). This could be an indication of photospheric heating by grains (Tsuji et al. 1996a) which tend to bring the spectral distribution closer to a simple thermal radiation, i.e., a blackbody. In such case, Gl 229B would have to be much cooler than derived with our grainless models in order to exhibit the observed water and methane features. This would imply an age for the system in conflict with the present estimate (see § 4 below). Effectively, a parallel investigation by Tsuji et al. (1996b) failed to reproduce the spectral distribution of Gl 229B using homogeneous dusty models, leading the authors to suggest that dust, rather than being distributed homogeneously with the gas in the brown dwarf regime, gathers in dust clouds. Another possibility is that grains could sink below the photosphere while the shrinking convection zone is no longer able to return this material to the surface.

In either case, this leads to reduced photospheric abundances as observed in Gl 229B *without* the expected greenhouse effect of grains upon the photosphere. To gauge the effects of condensation on our models and the atmospheric parameters we infer from them, we have recomputed the $T_{\rm eff} = 1000$ K, $\log g = 5.3$ model in the limiting case of Jovian abundances (C/O = 1.9 and nearly zero metallicity). While we found that decreased metallicity did improve the fit to the H bandpass and the $\lambda < 1.1$ μm region of the Gl 229B spectrum, it also slightly lowers the K-band flux relative to the J bandpass. Thus, a bluer $J - K$ color and a slightly higher gravity model are required to fit the spectrum, an effect which is, however, negligible compared to present uncertainties in the gravity estimates.

To be conservative, we set upper limits to the effective temperature and surface gravity of Gl 229B at $T_{\rm eff} = 1000$ K (based on the L' to N fluxes) and $\log g = 5.3 \pm 0.2$ (based on the relative K and J fluxes).

4. EVOLUTION AND MASS DETERMINATION

As brown dwarfs of increasing mass are more compact, hotter, and older at a given luminosity, the effective temperature and gravity derived in the previous section can help limit the allowed ranges of mass and age for Gl 229B. We have computed the time evolution of brown dwarfs from 0.02 to 0.065 $M_\odot$ with solar metallicity. Details of the input physics for the internal structure can be found in Baraffe et al. (1995) and Chabrier, Baraffe, & Plez (1996). The atmospheric structure is defined for temperatures down to $T_{\rm eff} = 900$ K by the models already described in § 2.

We determined a maximum temperature for Gl 229B of $T_{\rm eff} \sim 1000$ K. The latest estimate of its bolometric luminosity, corrected for the scattered light of the primary, using broad-band photometry out to about 10 μm and using a blackbody tail extrapolation to longer wavelengths, is $L \sim 6.4 \times 10^{-6}\ L_\odot$ (Matthews et al. 1996). Also, the properties of the primary, Gl 229A, can be used to constrain the age of the binary (cf. Nakajima et al. 1995). Its kinematics suggest that the dM1 star belongs to the young disk population, even though the absence of Hα emission excludes a very young age. However, the detection of Hα absorption, which we were able to confirm in the Keck spectra of Gl 229A by G. Marcy and G. Basri (private communication), may also rule out a very old object (see, e.g., Reid, Hawley, & Mateo 1995). This is supported by the metal-rich properties deduced from photometry (cf. Leggett 1992). Independently, the photometric properties of the primary, Gl 229A ($M_V = 9.33$ and $V - I = 2.0$, $I - K = 1.96$; cf. Leggett 1992), are accurately reproduced by a $\sim$0.6 $M_\odot$ star as modeled by Chabrier et al. (1996). Between 0.5 and 5 Gyr, the main-sequence location of a 0.57 $M_\odot$ star with solar metallicity corresponds to $M_V \sim 9.30$ and $V - I = 1.90$, $I - K = 1.94$. We thus restrict our study to a time interval of 0.5–5 Gyr.

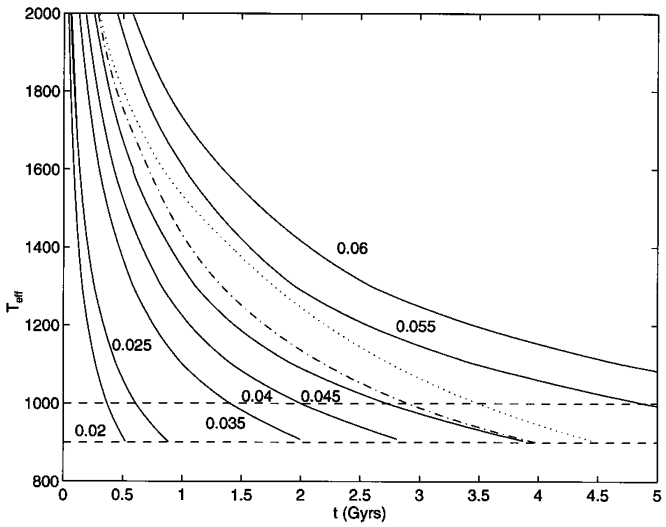

FIG. 3.—Effective temperature as a function of time for the indicated masses (in $M_\odot$). The dash-dotted line corresponds to a 0.045 $M_\odot$ model based on gray atmosphere including grain absorption, and the dotted line gives the grainless gray counterpart. The dashed horizontal lines give the $T_{\rm eff}$ range determined by the present spectral analysis.

Figure 3 shows the evolution of the effective temperature for different masses as a function of age. In the age range specified above, the only masses compatible with the temperature limit set by the synthetic spectral analysis lie between 0.02 and 0.055 $M_\odot$. The high sensitivity of the gravity to the mass at a given temperature can be used to narrow the mass range further. In Figure 4 we plot the variation of the surface gravity $g = GM/R^2$ as a function of $T_{\rm eff}$ for the same masses as in Figure 3. The best fits from the spectral analysis are also shown in this figure, with an uncertainty on the gravity of ± 0.2 (cf. § 3.2). For the temperature limit, $T_{\rm eff} = 1000$ K and $\log g = 5.3 \pm 0.2$, our favored choice (see § 3.1), the mass range is now reduced to 0.04–0.055 $M_\odot$. We also show our results for the pairing $T_{\rm eff} = 900$ K, $\log g = 4.8 \pm 0.2$, which yields 0.02–0.035 $M_\odot$. An examination of Figures 3 and 4 reveals that a gravity of $\log g < 4.5$ with $T_{\rm eff} = 900$ K would yield ages too low ($\tau < 5 \times 10^8$ yr) for the system. For completeness, the characteristics of our model brown dwarfs at each mass in the

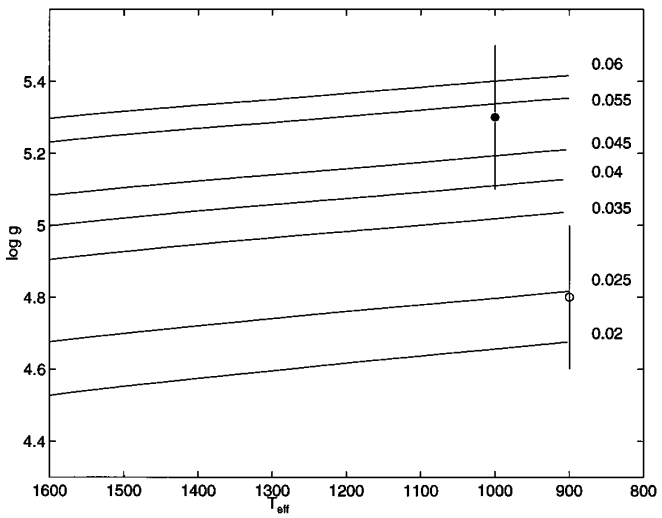

FIG. 4.—Gravity as a function of $T_{\rm eff}$. The circles give the best fit deduced from the synthetic spectra analysis, with an estimated theoretical error bar log $g \approx \pm 0.2$. ($T_{\rm eff} = 1000$ K, log $g = 5.3$ [*filled circle*]; $T_{\rm eff} = 900$ K, log $g = 4.8$ [*open circle*]).

entire grid with $T_{\rm eff} = 1000$ and 900 K are given in Table 1. Note that the observed important blueshift, due to CH_4 opacities in the K bandpass, characteristic of the transition "from the stellar to the substellar" domain is qualitatively reproduced by the models.

In order to estimate the effect of grain formation on the brown dwarf cooling, we have recomputed the evolutionary models based on a gray atmosphere using the Alexander & Ferguson (1994) opacities with and without grains (D. A. Alexander, private communication). As shown by Burrows et al. (1993) and Chabrier et al. (1996), the luminosity drops substantially when the location of grain formation reaches the bottom of the photosphere. Therefore, the grainless model will evolve at higher L and $T_{\rm eff}$. We find that, at a given age, the differences between models with and without grains are ~100 K in $T_{\rm eff}$ and ~25% in L in the temperature range of interest. This is illustrated in Figure 3 for the 0.045 $M_\odot$ model. Note that, for the previously determined temperature range, grainless nongray models predict an evolution similar to that predicted by gray models including grain formation, and thus yield similar mass determinations (see, e.g., Burrows et al. 1993, Fig. 4). Although the effect of grain formation on evolution might be more important when nongray model atmospheres are used, the present analysis based on gray atmosphere models changes the results by only ~0.01 $M_\odot$.

TABLE 1

CHARACTERISTICS OF BROWN DWARFS FOR [M/H] = 0

$M/M_\odot$	$T_{\rm eff}$ (K)	Age (Gyr)	$L/L_\odot$	log g	M_K	$J-K$[a]
0.02	1000	0.37	−4.97	4.66	14.51	0.75
	900	0.522	−5.17	4.67	15.36	0.44
0.025...	1000	0.61	−5.01	4.80	14.69	0.64
	900	0.88	−5.22	4.82	15.58	0.29
0.035...	1000	1.43	−5.10	5.02	15.07	0.42
	900	1.99	−5.27	5.04	15.87	0.09
0.04	1000	2.03	−5.13	5.11	15.22	0.33
	900	2.81	−5.31	5.13	16.02	−0.01
0.045...	1000	2.74	−5.16	5.19	15.33	0.25
	900	3.87	−5.35	5.21	16.21	−0.12
0.055...	1000	4.88	−5.21	5.34	15.58	0.10
	900	6.88	−5.41	5.35	16.51	−0.31
0.06	1000	6.59	−5.24	5.40	15.69	0.03
	900	9.23	−5.43	5.42	16.62	−0.38
0.065...	1000	10	−5.26	5.46	15.80	−0.04
	900	13.9	−5.46	5.47	16.72	−0.44

[a] Synthetic photometry on the Johnson-Glass system as in AH95. On this system, the Hale spectrum of Gl 229B gives $J-H = -0.115$, $H-K = -0.130$, and $J-K = -0.245$ for the brown dwarf.

5. DISCUSSION AND CONCLUDING REMARKS

We have used preliminary grainless model atmospheres to model the spectral distribution of cool brown dwarfs and found that these reproduce well the observed spectroscopic and photometric properties of Gl 229B. We confirm the presence of methane absorption bands and therefore the substellar nature of Gl 229B. The absence of CO absorption in the 4–5 μm range sets a secure upper limit of 1000 K on the effective temperature. Gravity can be constrained at fixed temperature using the relative K- to J-band fluxes, and this leads to values ranging from log $g = 5.3$ at 1000 K to log $g = 4.8$ at $T_{\rm eff} = 900$ K. A minimum temperature and gravity can be set by the presence of water vapor bands in Gl 229B's spectrum to about 700–800 K, where photospheric temperatures are expected to drop below the condensation temperature of H_2O.

While uncertainties in the age of the system and in the temperature of Gl 229B yield some indetermination for the mass of Gl 229B, we can derive upper limits from the effective temperature limit, namely, $M \leq 0.065\ M_\odot$ for an age $t \leq 10$ Gyr, and $M \leq 0.055\ M_\odot$ for a more likely age $t \leq 5$ Gyr. The most likely solution, $M \approx 0.04-0.055\ M_\odot$, is supported by the quality of the most reliable fit to the water bands for these parameters, and would be consistent with an age similar to that of our solar system. Our analysis cannot, however, exclude a mass as low as 0.02 $M_\odot$ if $T_{\rm eff} = 900$ K and $t = 0.5$ Gyr.

One of the main sources of uncertainty in the present models is the absence of grain formation in the computed atmospheres. Recent work by Tsuji et al. (1996a, 1996b) shows that grain formation may lead to substantial heating of the photospheres of cool M dwarfs and brown dwarfs, possibly resulting in a much lower effective temperature for Gl 229B than is derived with the present grainless models. The absence of predicted VO and FeH features in the red spectrum (Z band) of Gl 229B indicates reduced abundances of grain-forming elements, and therefore the presence of condensation and perhaps grain heating in this cool brown dwarf. However, homogeneous dusty models by Tsuji et al. (1996b) failed to reproduce the spectral distribution of Gl 229B, while the present models reproduce the observed strengths of molecular features such as water vapor which would otherwise be substantially weakened by the greenhouse effect of grains. This suggests that Gl 229B's atmosphere is very reminiscent of that of Jupiter, in which condensed material and cloud-top layers were not found in the expected amounts by the *Galileo* atmospheric probe (D. Isbell & D. Morse, NASA press release 96-10). Perhaps in both Jupiter and Gl 229B, these condensates either formed in clouds or sank deeper into the atmosphere.

We thank T. Nakajima and colleagues for providing an updated version of the Gl 229B spectrum in electronic form, as well as the referee for his valuable comments. We are also indebted to J. M. Matthews and D. R. Alexander for proofreading the text. This research has been partially supported by NASA LTSA and ATP grants to ASU and an NSF grant AST-9217946 to WSU. The atmospheric calculations have been performed on the Cray C90 of the San Diego Supercomputer Center and on the IBM SP2 of the Cornell Theory Center, supported by the NSF.

REFERENCES

Alexander, D. R., & Ferguson, J. W. 1994, ApJ, 437, 879
Allard, F., & Hauschildt, P. H. 1995, ApJ, 445, 433 (AH95)
Allard, F., Hauschildt, P. H., Miller, S., & Tennyson, J. 1994, ApJ, 426, L39
Baraffe, I., Chabrier, G., Allard, F., & Hauschildt, P. H. 1995, ApJ, 446, L35
Burrows, A., Hubbard, W. B., Saumon, D., & Lunine, J. I. 1993, ApJ, 406, 158
Chabrier, G., Baraffe, I., & Plez, B. 1996, ApJ, 459, L91
Grevesse, N., & Noels, A. 1993, in Origin and Evolution of the Elements, ed. N. Prantzos, E. Vangioni-Flam, & M. Cassé (Cambridge: Cambridge Univ. Press), 14
Husson, N., Bonnet, B., Scott, N. A., & Chedin, A. 1992, J. Quant. Spectrosc. Radiat. Transfer, 48, 509
Irwin, A. W. 1988, ApJS, 74, 145
Jørgensen, U. G. 1994, A&A, 284, 179
Langhoff, S. R., & Bauschlicher, C. W. 1993, Chem. Phys. Lett., 211, 305
Leggett, S. K. 1992, ApJS, 82, 351
Matthews, K., Nakajima, T., Kulkarni, S. R., & Oppenheimer, B. R. 1996, in preparation
Miller, S., Tennyson, J., Jones, H. R. A., & Longmore, A. J. 1994, in IAU Colloq. 146, Molecular Opacities in the Stellar Environment, ed. P. Thejll & U. G. Jørgensen, (Copenhagen: Niels Bohr Inst. and NORDITA Press), 296
Nakajima, T., Oppenheimer, B. R., Kulkarni, S. R., Golimowski, D. A., Matthews, K., & Durrance, S. T. 1995, Nature, 378, 463
Neale, L., Miller, S., & Tennyson, J. 1996, ApJ, in press
Neale, L., & Tennyson, J. 1995, ApJ, 454, L169
Oppenheimer, B. R., Kulkarni, S. R., Nakajima, T., & Matthews, K. 1995, Science, 270, 1478
Reid, N., Hawley, S. L., & Mateo, M. 1995, MNRAS, 272, 828
Rothman, L. S., et al. 1992, J. Quant. Spectrosc. Radiat. Transfer, 48, 469
Schryber, H. S., Miller, S., & Tennyson, J. 1995, J. Quant. Spectrosc. Radiat. Transfer, 53, 373
Strong, K., Taylor, F. W., Calcutt, S. B., Remedios, J. J., & Ballard, J. 1993, J. Quant. Spectrosc. Radiat. Transfer, 50, 363
Tsuji, T., Ohnaka, K., & Aoki, W. 1996a, A&A, 305, L1
———. 1996b, preprint
Tyuterev, VL. G., et al. 1994, J. Quant. Spectrosc. Radiat. Transfer, 52, 459
Zheng, C., & Borysow, A. 1994, ApJ, 441, 960